



Published in final edited form as:

Radiother Oncol. 2019 December ; 141: 275–282. doi:10.1016/j.radonc.2019.07.010.

Multi-Institutional Evaluation of MVCT Guided Patient Registration and Dosimetric Precision in Total Marrow Irradiation: A Global Health Initiative by the International Consortium of Total Marrow Irradiation

Darren Zuro^{1,2}, Stefano Vagge³, Sara Broggi⁴, Stefano Agostinelli³, Yutaka Takahashi⁵, Jamison Brooks¹, Paulina Leszcynska⁶, An Liu¹, Claudio Zucchetti⁷, Simonetta Saldi⁸, Chunhui Han¹, Mauro Cattaneo⁴, Sebastian Giebel⁶, Marc Andre Mahe⁸, James F Sanchez¹, Parham Alaei², Chiara Anna⁴, Kathryn Dusenbery², Antonio Pierini⁹, Guy Storme¹⁰, Cynthia Aristei⁸, Jeffrey Y.C. Wong¹, Susanta Hui^{1,*}

¹Department of Radiation Oncology, Beckman Research Institute, City of Hope, Duarte, USA

²Department of Radiation Oncology, University of Minnesota, Minneapolis, USA

³Department of Medical Imaging and Radiation Sciences, IRCCS Ospedale Policlinico San Martino, Genoa, Italy

⁴Department of Medical Physics, San Raffaele Scientific Institute, Milan, Italy.

⁵Departments of Radiation Oncology, Osaka University, Suita, Osaka, Japan

⁶Department of Radiotherapy Planning, Maria Skłodowska-Curie Memorial Cancer Center and Institute of Oncology, Gliwice Branch, Poland

⁷Department of Radiation Oncology, University of Perugia, Perugia, Italy

⁸Department of Radiation Oncology, University of Nantes, Nantes, France

⁹Division of Hematology and Clinical Immunology, Department of Medicine, University of Perugia, Perugia, Italy

¹⁰Department of Radiotherapy UZ Brussel, Laarbeeklaan, 101, 1090-Brussel, Jette ,Belgium

Abstract

Purpose: Total Marrow Irradiation (TMI) is a highly conformal treatment of the human skeleton structure requiring a high degree of precision and accuracy for treatment delivery. Although many centers worldwide initiated clinical studies using TMI, currently there is no standard for pretreatment patient setup. To this end, the accuracy of different patient setups was measured using pretreatment imaging. Their impact on dose delivery was assessed for multiple institutions.

[§]**Corresponding Author:** Dr. Susanta K Hui, Professor, Department of Radiation Oncology, City of Hope National Medical Center, 1500 E Duarte Rd, Duarte, CA 91010, Tel. 626-218-0556, shui@coh.org.

Publisher's Disclaimer: This is a PDF file of an unedited manuscript that has been accepted for publication. As a service to our customers we are providing this early version of the manuscript. The manuscript will undergo copyediting, typesetting, and review of the resulting proof before it is published in its final form. Please note that during the production process errors may be discovered which could affect the content, and all legal disclaimers that apply to the journal pertain.

Methods and Materials: Whole body imaging (WBI) or partial body imaging (PBI) was performed using pretreatment megavoltage computed tomography (MVCT) in a helical Tomotherapy machine. Rigid registration of MVCT and planning kilovoltage computed tomography images were performed to measure setup error and its effect on dose distribution. The entire skeleton was considered the planning target volume (PTV) with five sub regions: head/neck (HN), spine, shoulder and clavicle (SC), and one avoidance structure, the lungs. Sixty-eight total patients (>300 images) across six institutions were analyzed.

Results: Patient setup techniques differed between centers, creating variations in dose delivery. Registration accuracy varied by anatomical region and by imaging technique, with the lowest to the highest degree of pretreatment rigid shifts in the following order: spine, pelvis, HN, SC, and lungs. Mean fractional dose was affected in regions of high registration mismatch, in particular the lungs.

Conclusions: MVCT imaging and whole body patient immobilization was essential for assessing treatment setup, allowing for the complete analysis of 3D dose distribution in the PTV and lungs (or avoidance structures).

Keywords

MVCT; TMI

INTRODUCTION

Total body irradiation (TBI) has been widely used for conditioning prior to hematopoietic stem cell transplantation (HCT). Dose escalation of TBI produces decreased relapse rates in patients with leukemia [1, 2]. However, treatment-related deaths increase because of organ toxicity from TBI [1, 2]. This outcome negates any potential advantage for survival with escalated doses of TBI. Recently, total marrow irradiation (TMI) was developed to achieve dose escalation with helical Tomotherapy [3-7] while reducing radiation doses to normal tissues. Unlike TBI, TMI targets the entire skeletal system while sparing sensitive, normal tissues, such as the lungs. TMI treatment risks are similar to those of intensity modulated radiation therapy (IMRT), such as sharp dose gradients near both the planning target volume (PTV) and avoidance structures. The close proximity of dose gradients to these structures increases the risk for detrimental impacts caused by patient positioning and setup uncertainties [8]. Reliable pre-treatment patient positioning methods along with accurate and precise verification of patient positioning are therefore crucial to deliver the prescribed dose to the PTV while sparing normal tissues.

Currently, there is a worldwide effort to adopt targeted radiation treatment procedures for hematological malignancies, and the potential for TMI is being studied at multiple centers globally [9, 10]. Many of these centers use different pre-treatment position verification techniques. Little is known about how the patient position varies across multiple treatment fractions or how patient positioning impacts TMI dose delivery between different centers. To investigate this unmet clinical need, the international consortium of total marrow irradiation (ICTMI) worked with the six participating institutions to assess the accuracy of patient setup and its impact on dose delivery. Two steps were taken to accomplish this goal: 1)

compare pre-treatment rigid registrations by institution to assess patient setup technique and 2) quantify how pretreatment rigid registration affects the planned dose delivered to the patient. On the basis of this evaluation, recommendations for improved TMI treatment setup are given.

METHODS AND MATERIALS

Patient Immobilization

All institutes used whole body immobilization with some minor variations in technique. Institutions 1, 3, 5, and 6 immobilized patients using a Vac-Lok and thermoplastic mask (each from different companies depending on the center) [3, 11]. TMI is typically treated in 2 parts: an upper (body) and lower (legs) section. Institution 1 used a breathing motion tracking software to account for chest motion. Institutions 2 and 4 used an all-in-one base plate comprising 2-3 thermoplastic meshes to restrict regions of the head/neck, thorax/arms, and legs [9]. For initial setup and verification, a series of tattoos along the head, shoulder, thorax, pelvis, and leg regions were used.

Definition of the CTV and PTV

For TMI, the clinical target volume (CTV) was marrow-containing bony skeleton. Strictly speaking, the entire bony skeleton is more than the marrow-forming tissue and therefore did not need to be entirely included in the CTV. However, for simplicity of contouring, it was easier to use the CT number of bone to define the CTV. For institution 3, instead of a uniformly symmetric margin, the planning target volume (PTV) was created from the CTV using a customized margin and is described as follows. For the areas that have more setup uncertainty such as shoulders and spinous processes, a 5-10 mm margin was added to CTV to generate PTV. For the arms and thighs, a 10 mm margin was used. For all other bones including skull, anterior spine and pelvic bones where setup is reproducible, no margin was used because the CTV was the bone, but the biologic target was the marrow. Institutions 1 & 2 used a symmetric 10 mm margin for all target regions. Institutes 4 & 6 used a symmetric 5 mm and 7 mm margin, respectively. Institute 5 had a customized PTV with margins of 5 mm to the long bone of the extremities, 3 mm for pelvis, 2 mm for cranial bones, and 1 mm for all other bones.

Planning Philosophy

We identified two different approaches for TMI treatment planning: conformal avoidance and conformal targeting, as described previously by Hui et al [11]. Conformal targeting focuses irradiation on the ribs and spares as much of the non-lung normal tissue as possible. Conformal avoidance irradiates the non-lung normal tissue to the prescribed dose, with a high dose interface at the boundary of the lungs. Institution 1 was the only institution to utilize conformal targeting, whereas the other institutions treated with conformal avoidance. To treat the legs, a second plan was created and the patient rotated to feet first supine and reimaged/treated [12] using the helical TomoTherapy.

Daily MVCT Imaging

Daily MVCT images and image registration data from 6 institutions and 68 total patients using different patient immobilizations, megavoltage computed tomography (MVCT) imaging protocols, and TMI treatment plans were acquired through the International Consortium of TMI (ICTMI) (Table 1). The data were collected using the helical Tomotherapy (Accuray Inc., Madison, WI) unit, which has an on-board MVCT detector array to generate volumetric images for patient localization [13]. Patient pretreatment setup is defined as the imaging, immobilization, and planning technique used for the delivery of the radiation therapy.

Two methods of pretreatment imaging were used: Whole body MVCT imaging (WBI) was used in institutions 1, 2, and 3, and partial body MVCT imaging (PBI) was used in institutions 4, 5, and 6 (Figure 1). Whole body images were taken from the top of the neck or base of the skull to below the pelvis (Figure 1a) and registered with the kVCT. Partial body imaging (PBI) techniques typically covered 2-3 regions. The first region started at the base of the skull down to the shoulders (Figure 1b). The second region covered the abdominal cavity down to the pelvis (Figure 1c). The third region covered the top of the iliac crest down to the diaphysis of the femur (Figure 1d). For PBI-based registrations, shifts from both the head and neck (HN) and lower regions were recorded and averaged together. The averaged coordinates were used as the pretreatment shifts for that fraction. Registration of the partial and whole body images and the potential for registration mismatches can be seen in Figures 1e-k for the different regions. MVCT slices with widths of 6 mm are commonly used to minimize time for patient scanning and post image processing. Before MVCT imaging, alignment with external lasers to fiducial markers on the patient is done by a therapist.

Pretreatment Rigid Registration Assessment and its Effect on Dose Recalculation

Pre-treatment rigid registrations from each institution were evaluated following previously published methods [7, 14, 15]. All CT images were down-sampled to 256x256 resolution to match TomoTherapy based MVCTs, ensuring that differences in resolution would not affect the dose calculation. Results from pre-treatment rigid registrations were used to quantify setup errors for each institution, which include global systematic error, random error, patient-to-patient variations, and the overall distribution error. Details of these error calculations can be found in the supplemental section.

Rigid registration dose (or delivered dose) was evaluated using the recorded pre-treatment shifts taken from the TomoTherapy MVCT image guidance system. The reported translational shifts were first applied between the planning KVCT and the daily MVCT, and then the daily fractional dose was calculated using the original DICOM-RTDose files. Since translation shifts were accounted for we are investigating the residual error from patient setup. All dose evaluations were performed within the Velocity AI system (Varian Medical Systems, Inc., Palo Alto, CA, USA). The planned dose distribution was compared with the delivered dose (sum of the fractional doses) in terms of a structure's mean dose, 90% (D90), and 10% (D10) isodose line. The relative difference in the planning dose per fraction was

evaluated for an overall assessment of treatment delivery accuracy. Both regional dose and overall skeletal dose variations were considered in treatment delivery assessment.

Statistical analyses were performed using GraphPad Prism v 7.04 (GraphPad Software Inc. La Jolla, CA, USA). Data are presented as the mean \pm s.d. Outliers were identified using a robust nonlinear regression method, ROUT (Q = 1%, “Q” is the maximum desired false discovery rate) and were assessed per institution. Multiple group comparisons were performed with a one-way ANOVA test correcting for multiple comparisons. Group comparisons were performed with an unpaired two-tailed Student’s test. A p value of < 0.05 was considered statistically significant.

RESULTS

Rigid Registration Errors

Measures of the mean, random, and systematic errors from pre-treatment patient setup are presented in Figures 2a-d for each institution, and a detailed chart of the errors is found in Supplement Table 1. As shown in Figure 2a, the highest global error is 8.2 mm, which was significantly different ($p < 0.0001$) from the other institutions. This result is largely due to the y-direction (longitudinal) error of 6.8 mm. Institution 5 was the best overall performing institution, with an overall distribution error of 4.5 mm compared to 7.3 mm. Results from WBI and PBI institutions for patient to patient and random error can be found in Figure 2e. The imaging techniques were found to be significant from each other ($p < 0.0001$) with WBI having the lower overall distribution error of 3.8 mm compared to PBI’s 5.3 mm. Patient roll was small (< 1 degree, Supplement Table 1) and therefore it is not included for dose calculation.

Effect of MVCT length on patient registration

Because PBI was used by half of the centers covering different anatomical regions with varying number of slices, we investigated whether there was a positive correlation between number of slices used for PBI registration and WBI registrations. The effect of varying the number of MVCT slices used for image registration on registration precision and accuracy are shown in Supplement S1. The magnitude of RMS displacement between WBI and PBI of varying slices decreased with increasing number of slices for both pelvis and lung regions. Our results indicate a suggested minimal regional coverage of > 10 cm in the cranial-caudal direction with a slice thickness of 5-6 mm to minimize spatial error of less than 5% from the overall WBI baseline registration.

Effects of rigid registration on dose

Figure 3 displays the percentage difference in mean dose for daily treatments for each WBI imaging institution. Percent differences from the planned and delivered doses for the PTV are in Figure 3a-e. Prescription dose is defined differently for each institution as seen in Table 1. Figure 3g-k displays the percent difference between the regional CTV mean dose and the planned PTV mean dose. Figure 3f is the 95% Confidence Intervals (CIs) for the PTV and are measured as $[-2.8\%, -1.3\%]$ in the HN, $[-1.3\%, -0.4\%]$ in the SC, $[-0.9\%, -0.3\%]$ in the spine, $[-1.2\%, -0.6\%]$ in the pelvis, and $[-2.0\%, -0.6\%]$ for the skeleton.

Figure 3l shows the 95% CIs for the mean CTV dose as compared with the mean PTV dose, measured as $[-3.0\%, -0.7\%]$ in the HN, $[-1.6\%, -0.4\%]$ in the SC, $[-0.7\%, -0.1\%]$ in the spine, $[-2.3\%, -0.4\%]$ in the pelvis, and $[-2.7\%, -1.0\%]$ for the skeleton. While institute 1 has higher uncertainty in D90 in skeleton; institutes 2 & 3 have higher uncertainties in the pelvis (Figure 3a).

Figure 4 displays the percentage mean lung dose difference for daily treatments for each WBI imaging institution. The different treatment planning isodose distributions are visualized in Figure 4b & 4c. The 95% CI for lungs from WBI institutes is $[-0.8\%, 3.4\%]$ as seen in Figure 4d. Figures 4e-j are the resulting dose volume histograms (DVHs) of the lungs for 3 different cases: high, close to expected, and low dose. Blue represents the resulting fractional dose and red the original planned dose. A representative fraction with shoulder misalignment and its effect on PTV dose can be seen in Figure 5.

DISCUSSION

This is the first multicenter investigation of the precision of TMI delivery through the ICTMI consortium. We performed analysis of pretreatment patient setup and its effect on the administered dose between multiple institutions using different setup methods. MVCT imaging was crucial to assess pretreatment patient setup, dose validation and institutional variations in dosimetric accuracy. Pretreatment WBI MVCT allows for assessment of 3D dose distribution within the skeletal PTV and lungs. Institutional variations in pretreatment patient setup existed with overall distribution errors ranging from 4.5 mm to 7.3 mm.

Pretreatment Rigid Registration Errors and their Effects on Dose Distribution

There are significant differences between institutions for patient pretreatment setup. The longitudinal (y) direction of rigid registration had the highest overall distribution error compared with the lateral (x) and vertical (z) directions (Supplement Table 1 and Figure 2a). These results are different from previous works which indicated greater error in the z direction [7, 15]. This difference is likely due to previous studies investigating patient setup for solid tumor treatments rather than whole body skeletal targeting. Most treatment protocols set a threshold for pre-treatment setup. For example, if the shifts are greater than 5 mm, the patient should be moved and reimaged. If pre-alignment is not properly performed, large displacements can be identified with MVCT imaging. In one institution, the vertical direction shifts were far outside expected values [>5 cm]. The pretreatment MVCT allows for detection of these large shifts, suggesting the need for image guidance with conformal radiation delivery.

The D90 had greatest uncertainty in skeletal regions as compared to the mean or D10. On the other hand, the lungs had the greatest uncertainty and dosimetric variation in D10 values. An example of these uncertainties can be seen in the DVH curves for a single patient treatment (Supplement Figure S2). In TMI studies, the DVH of skeletal target regions at the D90, and the lungs at D10, should be critically evaluated to minimize uncertainties to improve on the overall accuracy and precision of the treatment. Details of the CTV dosimetry can be found in the supplemental section.

Despite regional differences in the delivered dose, the overall PTV mean dose was still within 5% of the planned dose for all institutions. The example in Figure 5 shows the shoulder and clavicle (SC) were misaligned; however, the misalignment had no effect on the overall PTV dose for that day, because the SC only accounts for <2% of the total skeletal volume. However, in the case of non-homogeneous disease distribution (e.g. leukemia), small regions of poor dose coverage could have adverse effects on relapse prevention, demonstrating the importance of 3D DVH calculations of PTV dose [16-18]. 3D imaging of target and its localization may be important to avoid the possibility of under-dosing (cold spot) the target regions and to allow accurate dose delivery [16].

The merits of WBI imaging compared to PBI imaging

Among the participating centers, institution 5 had the lowest overall error when compared to the other institutions using PBI imaging. PBI is faster to assess patient positioning than WBI. However, PBI results in incomplete images of certain key regions such as the lung (Figure 1b & 1h), which may result in loss of information that is relevant to assess patient dose delivery. While the variation in systematic error between WBI and PBI is similar, the overall error distribution is less for WBI because of lower random error (Figure 2e & Supplement Table 2). One possibility for higher error in PBI is the averaging of multiple limited body registrations which are then applied as the overall rigid shifts. A limitation of MVCT imaging is poor soft tissue contrast. However, for TMI, MVCT imaging is useful for identifying bony treatment regions. Image resolution and the speed of MVCT imaging for TMI treatments are currently being improved, which has potential to further reduce image acquisition time, making WBI MVCT scans more feasible [19].

Lung dose and planning philosophy

One of the major goals in TMI planning is to limit the lung dose to reduce risk for interstitial pneumonitis (IP). Previous studies on IP from TBI-related radiation exposure to the lungs is directly associated with mean lung dose, dose per fraction, dose rate, and chemotherapy regimen [20, 21]. However, the lung dose measurements from these studies are obtained by single point dosimetry rather than calculated using 3D imaging based dosimetry, which makes variations in dose poorly understood [22]. WBI allows for 3D dosimetric analysis, which will enable quantitative associations between 3D dose distribution and IP.

There was greater uncertainty (nearly double) in the D10 for conformal targeting compared with conformal avoidance (Figure 4a). Variation in the lung dose is visible fraction to fraction, and often the deviation in the DVH occurs at a high dose as seen in Figure 4e-j. However, the mean dose for the whole lung was typically higher for conformal avoidance (0.5% from expected) versus conformal targeting (1.2% from expected) planning because of the presence of high dose interfaces in close proximity to the lung. One of the major goals of TMI clinical trials is to allow for dose escalation, as it has been shown to reduce the relapse rate [23-25]. Increasing accuracy of patient setup will enable further dose sparing to avoidance structures, enabling more reliable treatment delivery and dose escalation. Current prescriptions range from as low as 12Gy to as high as 20 Gy given in 2-4 Gy fractions. In the future, with increasing number of centers adopting TMI for treating hematological malignancies and experience gained from the current study, we will expand this study to a

larger population through the consortium to develop a more robust benchmark on setup and dosimetric tolerance. This approach could help to establish multicenter trials and compare clinical outcomes from different centers.

This work has shown that center-to-center variations in patient setup and doses delivered are dependent upon patient immobilization, pretreatment imaging protocols and PTV definition for TMI. The whole body immobilization is generally recommended for patient localization. The WBI MVCT imaging modality is recommended over PBI for monitoring patient setup variation. WBI MVCT imaging is also recommended for monitoring dose delivery. Based upon participating centers, PTV margin can be adjusted depending upon proximity of targets to OARs to improve dosimetric results, furthering the need for WBI before each treatment. Although this study suggests reasonable patient localization and dosimetry, further expansion is under way. As TMI treatment for bone marrow transplantation becomes more mainstream, additional centers can be added globally.

Supplementary Material

Refer to Web version on PubMed Central for supplementary material.

Acknowledgments

This work was supported by the National Institute of Health grants 1R01CA154491-01 and partially supported by the National Cancer Institute of the National Institutes of Health under award number P30CA033572. The content is solely the responsibility of the authors and does not necessarily represent the official views of the National Institutes of Health. The authors wish to thank Roberto Tarducci, Martina Iacco, and Krzysztof Slosarek for valuable discussions and support for this work.

References

1. Esiashvili N, et al. Higher Reported Lung Dose Received During Total Body Irradiation for Allogeneic Hematopoietic Stem Cell Transplantation in Children With Acute Lymphoblastic Leukemia Is Associated With Inferior Survival: A Report from the Children's Oncology Group. *Int J Radiat Oncol Biol Phys*, 2019.
2. Clift RA, et al. , Long-term follow-Up of a randomized trial of two irradiation regimens for patients receiving allogeneic marrow transplants during first remission of acute myeloid leukemia. *Blood*, 1998. 92(4): p. 1455–6. [PubMed: 9694737]
3. Wong JYC, et al. , Targeted total marrow irradiation using three-dimensional image-guided tomographic intensity-modulated radiation therapy: An alternative to standard total body irradiation. *Biology of Blood and Marrow Transplantation*, 2006. 12(3): p. 306–315. [PubMed: 16503500]
4. Wong JY, et al. , Image-guided total-marrow irradiation using helical tomotherapy in patients with multiple myeloma and acute leukemia undergoing hematopoietic cell transplantation. *Int J Radiat Oncol Biol Phys*, 2009. 73(1): p. 273–9. [PubMed: 18786784]
5. Han C, Schultheiss TE, and Wong JY, Dosimetric study of volumetric modulated arc therapy fields for total marrow irradiation. *Radiother Oncol*, 2012. 102(2): p. 315–20. [PubMed: 21724284]
6. Schultheiss TE, et al. , Image-guided total marrow and total lymphatic irradiation using helical tomotherapy. *International Journal of Radiation Oncology Biology Physics*, 2007. 67(4): p. 1259–1267.
7. Hui SK, et al. , Three-dimensional patient setup errors at different treatment sites measured by the Tomotherapy megavoltage CT. *Strahlenther Onkol*, 2012. 188(4): p. 346–52. [PubMed: 22398931]
8. Manning MA, et al. , The effect of setup uncertainty on normal tissue sparing with IMRT for head-and-neck cancer. *International Journal of Radiation Oncology Biology Physics*, 2001. 51(5): p. 1400–1409.

9. Corvo R, et al. , Helical tomotherapy targeting total bone marrow after total body irradiation for patients with relapsed acute leukemia undergoing an allogeneic stem cell transplant. *Radiotherapy and Oncology*, 2011. 98(3): p. 382–386. [PubMed: 21339008]
10. Engellau J, et al. , Implementation of Total Marrow Irradiation With Helical Tomotherapy; Clinical Experiences and Report on Organ Sparing in Pediatric Patients. *International Journal of Radiation Oncology Biology Physics*, 2018. 101(4): p. 1006–1007.
11. Hui SK, et al. , Feasibility study of helical tomotherapy for total body or total marrow irradiation. *Medical Physics*, 2005. 32(10): p. 3214–3224. [PubMed: 16279075]
12. Zeverino M, et al. , Advances in the implementation of helical tomotherapy-based total marrow irradiation with a novel field junction technique. *Med Dosim*, 2012. 37(3): p. 314–20. [PubMed: 22326734]
13. Ruchala KJ, et al. , Megavoltage CT image reconstruction during tomotherapy treatments. *Phys Med Biol*, 2000. 45(12): p. 3545–62. [PubMed: 11131183]
14. Yan D, et al. , Adaptive modification of treatment planning to minimize the deleterious effects of treatment setup errors. *Int J Radiat Oncol Biol Phys*, 1997. 38(1): p. 197–206. [PubMed: 9212024]
15. Schubert LK, et al. , A comprehensive assessment by tumor site of patient setup using daily MVCT imaging from more than 3,800 helical tomotherapy treatments. *Int J Radiat Oncol Biol Phys*, 2009. 73(4): p. 1260–9. [PubMed: 19251098]
16. Tome WA and Fowler JF, On cold spots in tumor subvolumes. *Medical Physics*, 2002. 29(7): p. 1590–1598. [PubMed: 12148742]
17. Mackie TR, et al. , Image guidance for precise conformal radiotherapy. *International Journal of Radiation Oncology Biology Physics*, 2003. 56(1): p. 89–105.
18. Vanderhoek M, et al. , Early assessment of treatment response in patients with AML using [(18)F]FLT PET imaging. *Leuk Res*, 2011. 35(3): p. 310–6. [PubMed: 20832860]
19. Magome T, et al. , Fast Megavoltage Computed Tomography: A Rapid Imaging Method for Total Body or Marrow Irradiation in Helical Tomotherapy. *Int J Radiat Oncol Biol Phys*, 2016. 96(3): p. 688–95. [PubMed: 27681766]
20. Sampath S, Schultheiss TE, and Wong J, Dose response and factors related to interstitial pneumonitis after bone marrow transplant. *Int J Radiat Oncol Biol Phys*, 2005. 63(3): p. 876–84. [PubMed: 16199317]
21. Gao RW, et al. , Influence of Total Body Irradiation Dose Rate on Idiopathic Pneumonia Syndrome in Acute Leukemia Patients Undergoing Allogeneic Hematopoietic Cell Transplantation. *Int J Radiat Oncol Biol Phys*, 2019. 103(1): p. 180–189. [PubMed: 30205123]
22. Hui SK, et al. , CT-based analysis of dose homogeneity in total body irradiation using lateral beam. *J Appl Clin Med Phys*, 2004. 5(4): p. 71–9.
23. Stein A, et al. , Phase I Trial of Total Marrow and Lymphoid Irradiation Transplantation Conditioning in Patients with Relapsed/Refractory Acute Leukemia. *Biol Blood Marrow Transplant*, 2017. 23(4): p. 618–624. [PubMed: 28087456]
24. Hui S, et al. , Dose Escalation of Total Marrow Irradiation in High-Risk Patients Undergoing Allogeneic Hematopoietic Stem Cell Transplantation. *Biol Blood Marrow Transplant*, 2017. 23(7): p. 1110–1116. [PubMed: 28396164]
25. Wong JY, et al. , Dose escalation of total marrow irradiation with concurrent chemotherapy in patients with advanced acute leukemia undergoing allogeneic hematopoietic cell transplantation. *Int J Radiat Oncol Biol Phys*, 2013. 85(1): p. 148–56. [PubMed: 22592050]

Highlights

- WBI institutions have lower overall setup error compared with PBI
- MVCT WBI ensures accurate assessment of 3D regional and global dose variations
- Variation is greatest in DVH of skeletal target at 90% and the lung at 10% isodose
- Dose planning (avoidance vs targeting) has significant impact on lung dose coverage

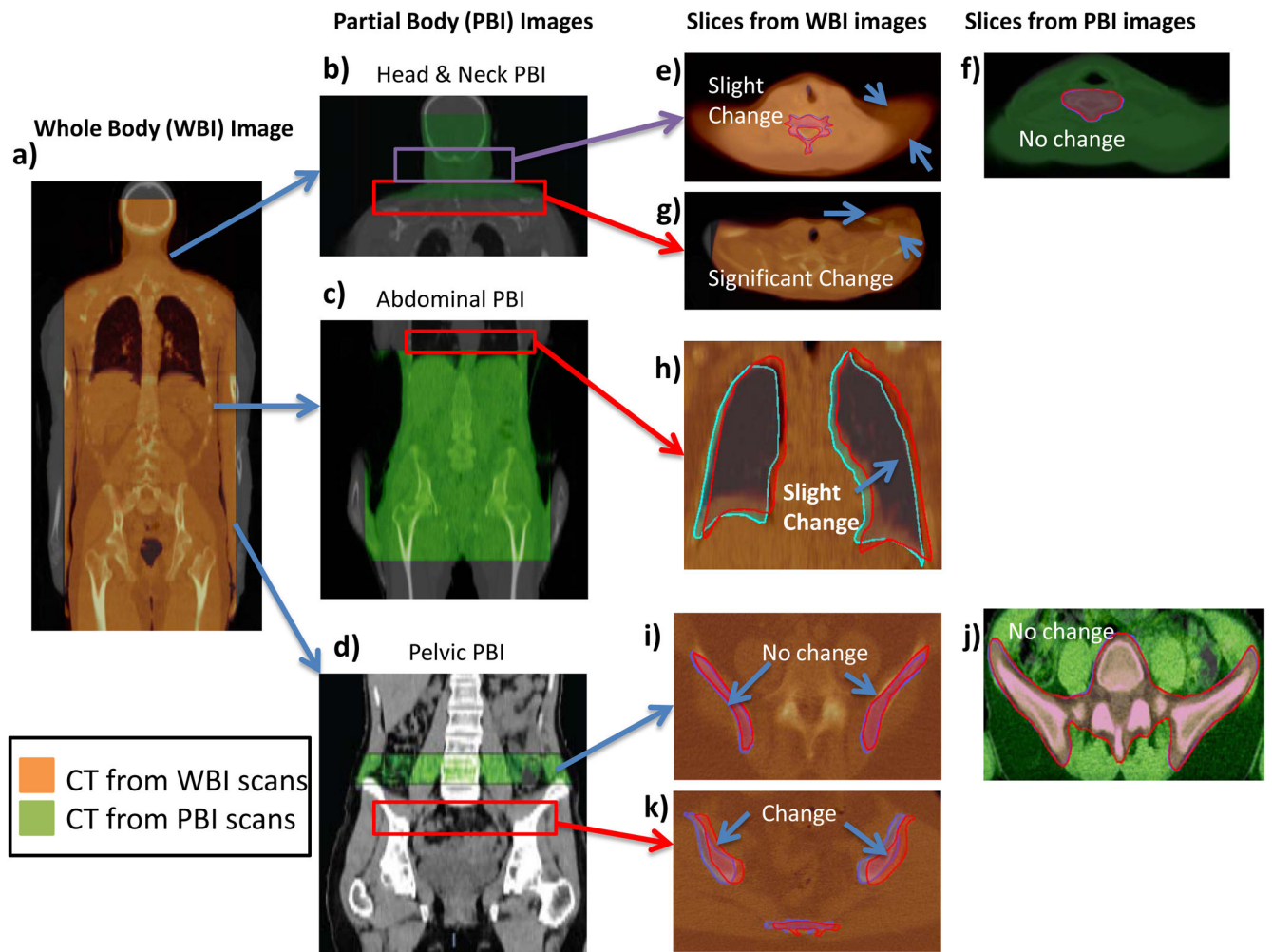


Fig. 1. Examples of WBI and PBI and their respective registrations. (a) Whole Body registration with associated kVCT. Three sub-regions commonly imaged in PBI: (b) head and neck. (c) abdominal, and (d) pelvic are shown registering with their kVCTs. Red boxes indicate regions where PBI was not performed but significant mismatches in WBI were found. Slices from WBI and PBI are shown for various regions (e–k). Orange CT scans are from WBI scans. Green CT scans are from PBI scans. Regions outside of PBI imaging show mismatch in WBI while only slight mismatches occur in nearby PBI images regions.

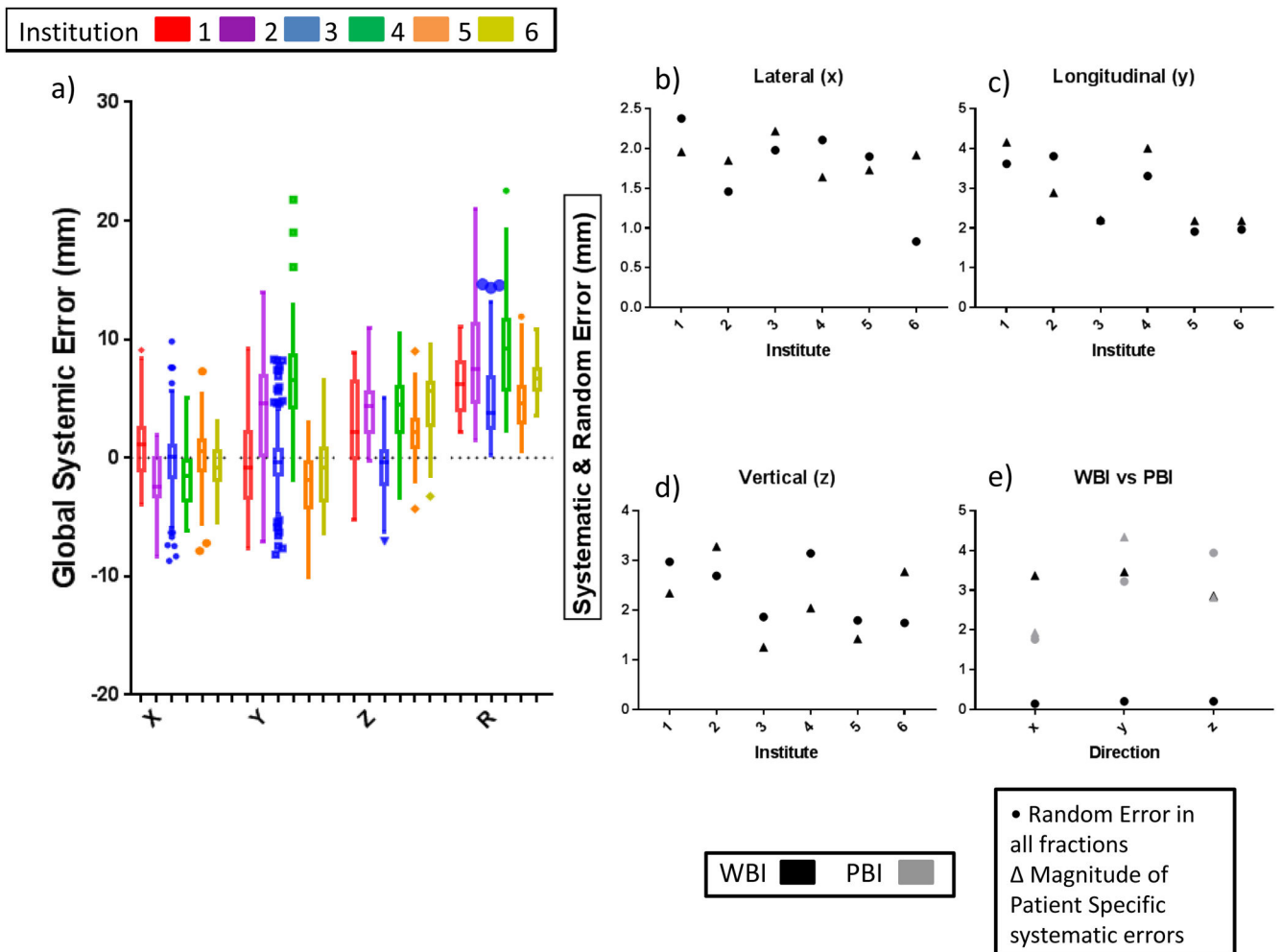


Fig. 2. (a) Box plot (Tukey) of rigid translations for each institution from pre-treatment rigid registration for each cardinal direction and the R (RMS average: $\sqrt{X^2 + Y^2 + Z^2}$). (b-d) Graph of random and systemic errors for each institution (x , y , z) in each cardinal direction (x , y , z). (e) Graph of random and systemic errors for the two primary MVCT imaging techniques: WBI & PBI for each cardinal direction. Numerical results can be found in Supplement Table 1 & 2. Results were calculated following Yan's methods and detailed in the Supplement section.

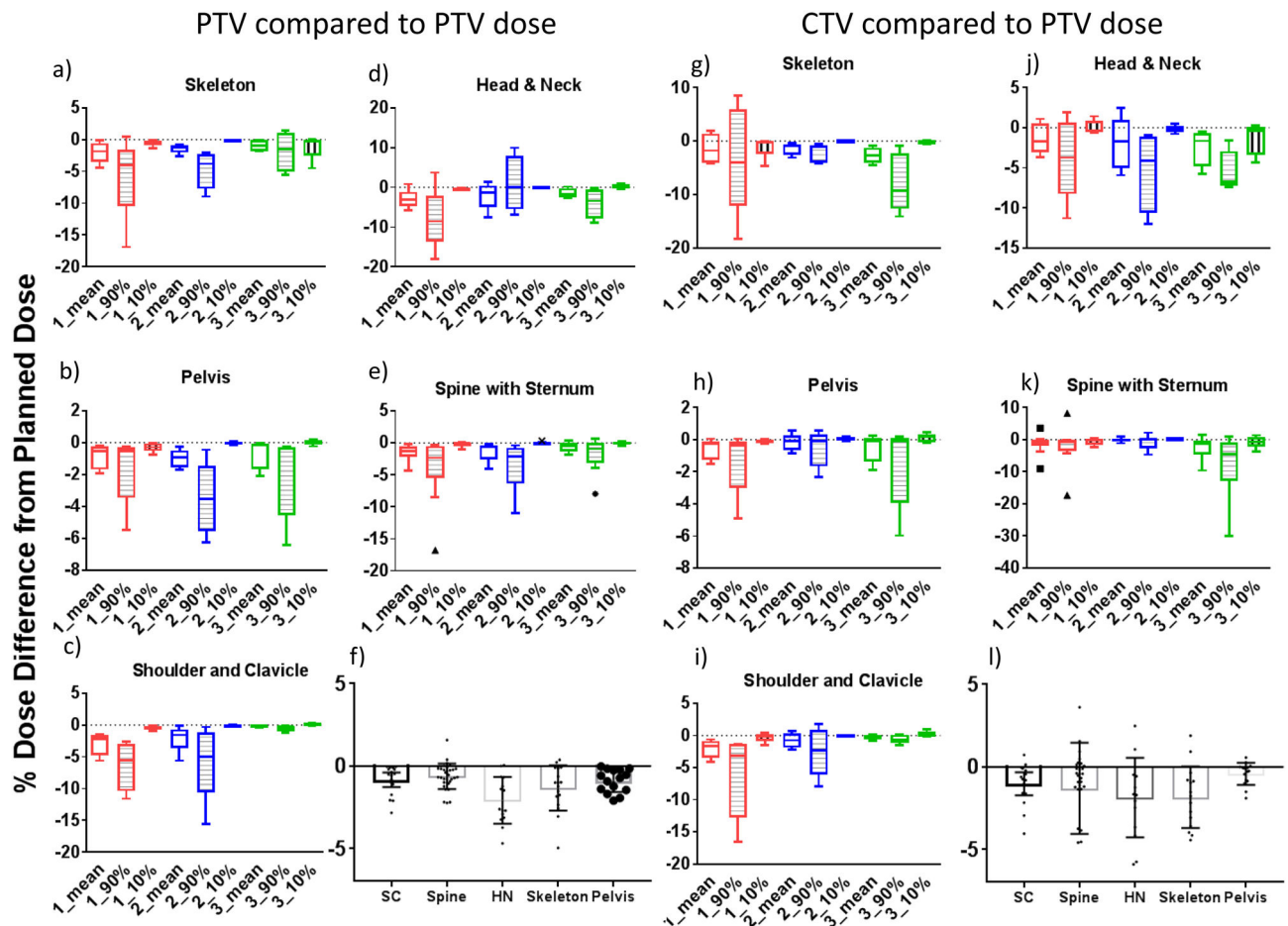


Fig. 3.

(a–e) Regional percent dose difference for the PTV between the delivered and the planned mean doses. 90% isodose (D90) and 10% isodose (D10) for the skeleton five sub regions: skeleton, head & neck (HN), shoulder with clavicle (SC). Spine with Sternum, and Pelvis, for all Whole Body imaging institutions 1, 2, & 3 ($N = 5$ for each institute). (g–k) Regional percent dose differences for the CTV as compared to the PTV mean dose. Delivered doses are calculated on the basis of recorded pretreatment shifts before radiation delivery. Regional percent differences in mean dose between (f) delivered PTV and (l) delivered CTV doses from the planned PTV mean dose in the SC, spine, head and neck (HN) based on the number of patients, presented with confidence intervals.

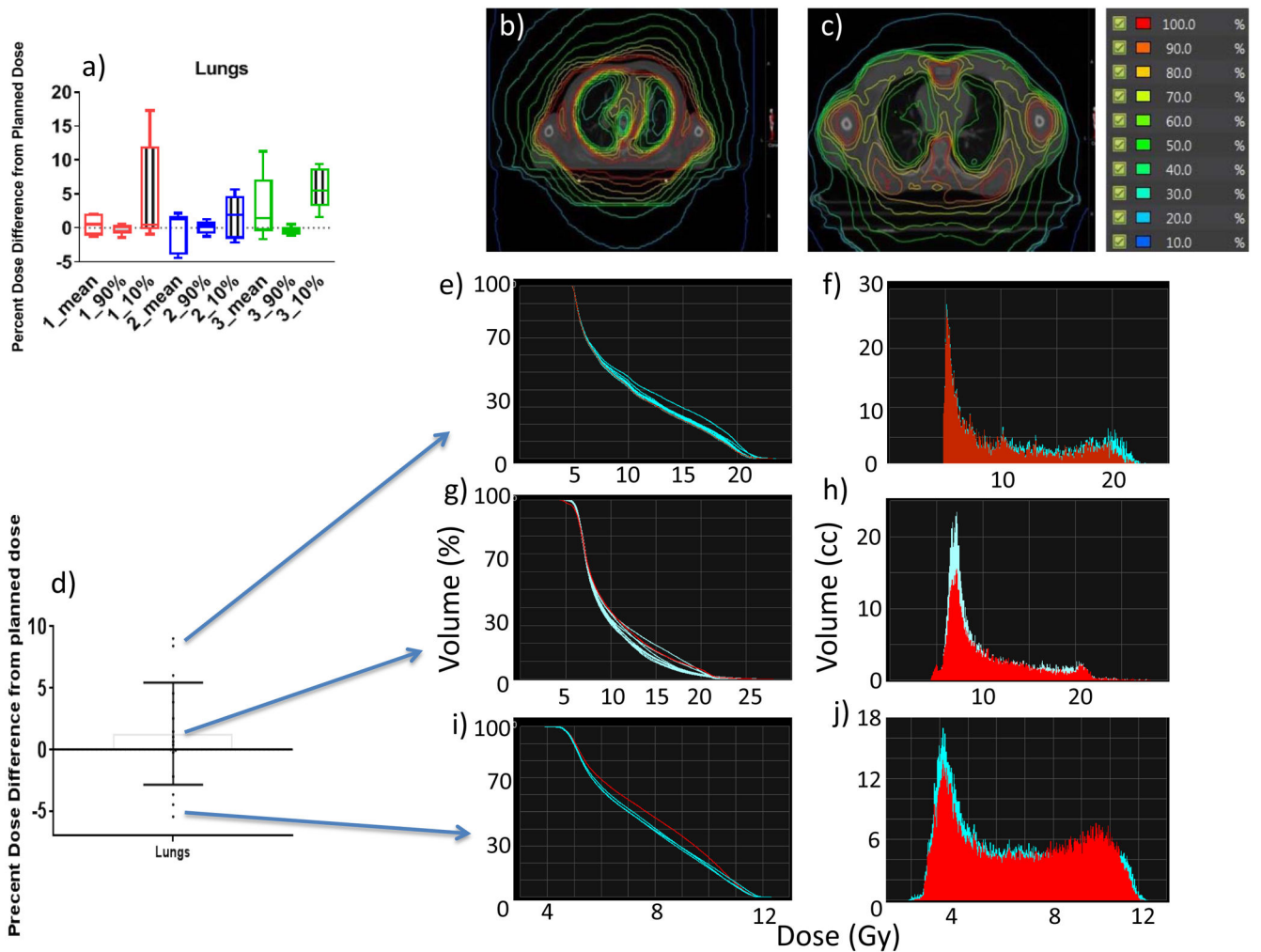


Fig. 4. (a) Percent dose difference for the lungs between delivered and planned mean doses, 90% isodose (D90) and 10% isodose (D10). Isodose lines of the thoracic cavity of two different treatment planning methods: (b) conformal avoidance and (c) conformal targeting. (d) Percent dose difference between expected and delivered dose in the lung for all WBI institutes ($N=15$) (e–j) is the resulting DVHs of the lung for 3 different representative cases: overdose, close to expected dose, and under-dosed. Blue represents the resulting fractional dose and red the original planned dose.

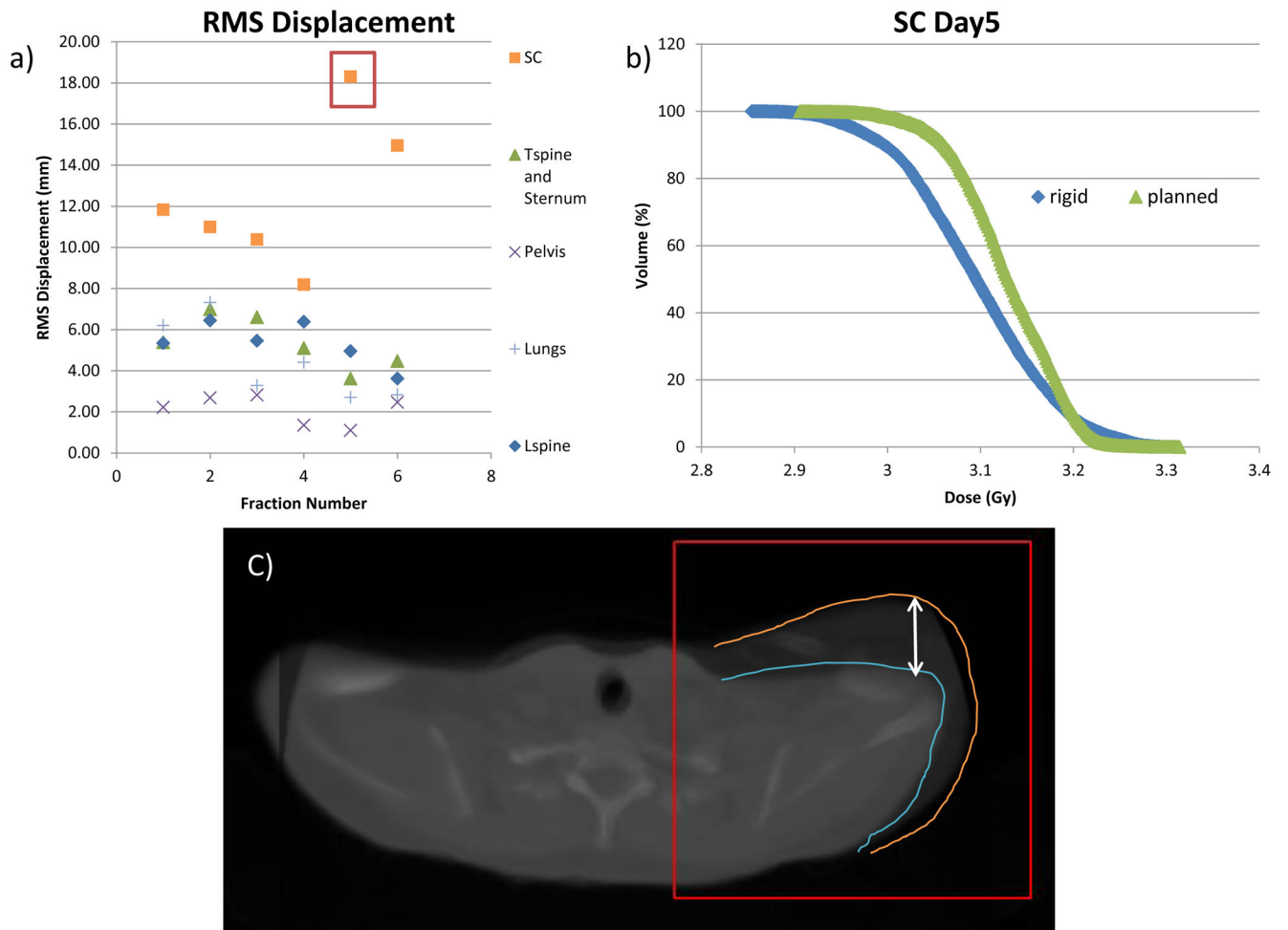


Fig. 5. Example of misaligned shoulder from TMI treated patient. (a) root-mean-square (RMS) displacement per fraction showing a large shift in the SC region on days 5 and 6. ($RMS = \sqrt{X^2 + Y^2 + Z^2}$), and (b) dose-volume-histogram (DVH) graph of the rigid and planned dose of the shoulder, for day 5 of treatment (c) image of misaligned shoulder on day 5 of treatment.

Table 1:

Classification of MVCT protocol, KVCT protocol, dose prescription and PTV definition per institution. Further details of PTV definition for institution 3 and 5 are provided in the methods section.

Institution	# of patients	PTV Definition	KVCT data	MVCT data	PTV Planned Dose
1	6	Symmetric 10mm margin	5mm thick slices, 108cm starting from bottom of pelvis	WBI , range of 0-6mm with a mean of 3mm thick slices, starting from bottom of pelvis	15-18 Gy in 5 - 6 fractions
2	11	Symmetric 10mm margin	10mm thick slices, 126cm scan length starting from the top of the head	WBI , 6mm thick slices, 80cm scan length, starting from top of the head	12Gy in 3 fractions
3	20	Non-symmetric margins variable for target region (see methods for details)	5mm thick slices, 121cm starting from the top of the head	WBI , 6mm thick slices, 80cm scan length, starting from top of the head	20Gy in 10 fractions
4	11	Symmetric 5mm margin	10mm thick slices, 134cm scan length starting from the top of the head	PBI , two sets of images taken at: 1. center of the pelvis 2. from the neck; 6mm thick slices with a scanning length 30cm each	8-12Gy in 4-7 fractions
5	10	Symmetric margins variable for target regions (see methods for details)	10mm thick slices, 134cm scan length starting from the top of the head	PBI , two sets of images taken at: 1. center of the pelvis 2. from the neck; 6mm thick slices with a scanning length 30cm each	13.5Gy in 9 fractions
6	10	Symmetric 7mm margin	2mm thick slices, 185cm scan length starting from the top of the head	PBI , two sets of images taken at: 1. iliac crest of the pelvis 2. midline of the eyes; 6mm thick slices with a scanning length 44cm each	12Gy in 3 fractions